JACC: CARDIOVASCULAR IMAGING
© 2019 BY THE AMERICAN COLLEGE OF CARDIOLOGY FOUNDATION
PUBLISHED BY ELSEVIER

VOL. 12, NO. 12, 2019

ORIGINAL RESEARCH

Dynamic Stress Computed Tomography Perfusion With a Whole-Heart Coverage Scanner in Addition to Coronary Computed Tomography Angiography and Fractional Flow Reserve Computed Tomography Derived

Gianluca Pontone, MD, PhD,[a] Andrea Baggiano, MD,[a] Daniele Andreini, MD, PhD,[a,b] Andrea I. Guaricci, MD,[c] Marco Guglielmo, MD,[a] Giuseppe Muscogiuri, MD,[a] Laura Fusini, MD,[a] Margherita Soldi, MD,[b] Alberico Del Torto, MD,[b] Saima Mushtaq, MD,[a] Edoardo Conte, MD,[a] Giuseppe Calligaris, MD,[a] Stefano De Martini, MD,[a] Cristina Ferrari, MD,[a] Stefano Galli, MD,[a] Luca Grancini, MD,[a] Paolo Olivares, MD,[a] Paolo Ravagnani, MD,[a] Giovanni Teruzzi, MD,[a] Daniela Trabattoni, MD,[a] Franco Fabbiocchi, MD,[a] Piero Montorsi, MD,[a,b] Mark G. Rabbat, MD,[d,e] Antonio L. Bartorelli, MD,[a,f] Mauro Pepi, MD[a]

ABSTRACT

OBJECTIVES The aims of the study were to test the diagnostic accuracy of integrated evaluation of dynamic myocardial computed tomography perfusion (CTP) on top of coronary computed tomography angiography (cCTA) plus fractional flow reserve computed tomography derived (FFR_{CT}) by using a whole-heart coverage computed tomography (CT) scanner as compared with clinically indicated invasive coronary angiography (ICA) and invasive fractional flow reserve (FFR).

BACKGROUND Recently, new techniques such as dynamic stress computed tomography perfusion (stress-CTP) emerged as potential strategies to combine anatomical and functional evaluation in a one-shot scan. However, previous experiences with this technique were associated with high radiation exposure.

METHODS Eighty-five consecutive symptomatic patients scheduled for ICA were prospectively enrolled. All patients underwent rest cCTA followed by stress dynamic CTP with a whole-heart coverage CT scanner (Revolution CT, GE Healthcare, Milwaukee, Wisconsin). FFR_{CT} was also measured by using the rest cCTA dataset. The diagnostic accuracy to detect functionally significant coronary artery disease (CAD) in a vessel-based model of cCTA alone, cCTA+FFR_{CT}, cCTA+CTP, or cCTA+FFR_{CT}+CTP were assessed and compared by using ICA and invasive FFR as reference. The overall effective dose of dynamic CTP was also measured.

RESULTS The prevalence of obstructive CAD and functionally significant CAD was 77% and 57%, respectively. The sensitivity and specificity of cCTA alone, cCTA+FFR_{CT}, and cCTA+CTP were 83% and 66%, 86% and 75%, and 73% and 86%, respectively. Both the addition of FFR_{CT} and CTP improves the area under the curve (AUC: 0.876 and 0.878, respectively) as compared with cCTA alone (0.826; $p < 0.05$). The sequential strategy of cCTA+FFR_{CT}+CTP showed the highest AUC (0.919; $p < 0.05$) as compared with all other strategies. The mean effective radiation dose (ED) for cCTA and stress CTP was 2.8 ± 1.2 mSv and 5.3 ± 0.7 mSv, respectively.

CONCLUSIONS The addition of dynamic stress CTP on top of cCTA and FFR_{CT} provides additional diagnostic accuracy with acceptable radiation exposure. (J Am Coll Cardiol Img 2019;12:2460–71) © 2019 by the American College of Cardiology Foundation.

ISSN 1936-878X/$36.00

https://doi.org/10.1016/j.jcmg.2019.02.015

Coronary computed tomography angiography (cCTA) was introduced as an anatomic imaging method to rule out the presence of coronary artery disease (CAD) (1) and also for improving prognostic assessment above baseline risk factor evaluation and functional stress test findings (2,3). However, despite its high negative predictive value, several factors limit its specificity and positive predictive value (4). To this regard, there is an emerging literature testing the addition value of traditional stress imaging test (5) or more recently of stress myocardial perfusion using computed tomography (CTP) and fractional flow reserve computed tomography derived (FFR_{CT}) on top of cCTA (5). Initial single-center studies with stress dynamic CTP testing its diagnostic accuracy and the additional value to cCTA and FFR_{CT} were mainly performed (6–18) with shuttle-mode approach. To the best of our knowledge, previous studies performing stress dynamic CTP with whole-heart coverage computed tomography (CT) scanner are missing. The aim of our study was to test the diagnostic accuracy of an integrated evaluation of dynamic CTP in addition to cCTA and FFR_{CT} compared with invasive coronary angiography (ICA) plus clinically indicated invasive fractional flow reserve (FFR) by using this new technology.

SEE PAGE 2472

METHODS

Patients scheduled for ICA between June 2017 and June 2018 were prospectively screened. Exclusion criteria included the following: 1) low to intermediate pre-test likelihood of CAD (<50%) (19); 2) previous history of revascularization or myocardial infarction; 3) acute presentation; 4) contraindication to contrast agent or impaired renal function; 5) contraindication to nitrates, beta-blockade, and/or adenosine; and 6) atrial fibrillation.

The institutional ethics committee approved the study protocol.

The study flow diagram is shown in **Figure 1** according to the STARD criteria (20).

PATIENT PREPARATION. For detailed description of patients, preparation, rest cCTA, and stress dynamic CTP scan protocol see the Supplemental Appendix. Patients were asked to refrain from smoking and caffeine for 24 h and fast for 6 h before the scan. All patients received sublingual nitroglycerine (2 puffs of 0.3 mg each). In patients with a resting heart rate (HR) >65 beats/min before the scan, metoprolol was administered intravenously with a titration dose up to 15 mg to achieve a target HR <65 beats/min. However, all patients were studied even if the target HR was not reached.

REST cCTA PERFORMANCE AND INTERPRETATION. We performed rest cCTA with a Revolution CT scanner (GE Healthcare, Milwaukee, Wisconsin) as previously described (21). All patients received a 70-ml bolus of iodixanol 320 (Visipaque 320 mg/ml, GE Healthcare, Oslo, Norway) at an infusion rate of 6.2 ml/s followed by 50 ml of saline solution at the same rate of infusion. Datasets of each cCTA examination were transferred to an image-processing workstation (Advantage Workstation 4.7, GE Healthcare, Milwaukee, Wisconsin) and independently analyzed according to the Society of Cardiovascular Computed Tomography guidelines for reporting (22) by 2 cardiac radiologists (M.G. and G.M.) who were blinded to the clinical history of the patients. Coronary arteries were segmented as suggested by the American Heart Association (23). Impaired image quality was classified according to the Likert score as previously described (4). The overall evaluability of cCTA was measured and the severity of the coronary lesions was categorized according to Society of Cardiovascular Computed Tomography guidelines for reporting (22). All non-evaluable coronary artery segments were censored as positive. Obstructive CAD was defined as the presence of stenosis >50%. A third cardiac radiologist with more than 5 years of experience in cCTA adjudicated the scores in cases of disagreement.

STRESS DYNAMIC cCTA PERFORMANCE AND INTERPRETATION. Twenty minutes after the cCTA, the stress acquisition was performed. Vasodilatation

ABBREVIATIONS AND ACRONYMS

AIF = arterial input function
AUC = area under the curve
CAD = coronary artery disease
cCTA = coronary computed tomography angiography
CT = computed tomography
CTP = computed tomography perfusion
ED = effective radiation dose
FFR = fractional flow reserve
FFR_{CT} = fractional flow reserve computed tomography derived
HR = heart rate
ICA = invasive coronary angiography
MBF = myocardial blood flow
PET = positron emission tomography
SPECT = single-photon emission computed tomography

From the [a]Centro Cardiologico Monzino, IRCCS, Milan, Italy; [b]Department of Cardiovascular Sciences and Community Health, University of Milan; [c]Institute of Cardiovascular Disease, Department of Emergency and Organ Transplantation, University Hospital "Policlinico" of Bari, Bari, Italy; [d]Loyola University of Chicago, Chicago, Illinois; [e]Edward Hines Jr. VA Hospital, Hines, Illinois; and the [f]Department of Biomedical and Clinical Sciences "Luigi Sacco", University of Milan, Milan, Italy. Dr. Pontone has received institutional research grant and/or speaker honorarium from General Electric, Bracco, Medtronic, Bayer, and Heartflow. Dr. Andreini has received institutional research grant and/or speaker honorarium from General Electric, Bracco, and Heartflow. All other authors have reported that they have no relationships relevant to the contents of this paper to disclose.

Manuscript received September 4, 2018; accepted February 1, 2019.

JACC: CARDIOVASCULAR IMAGING, VOL. 12, NO. 12, 2019
DECEMBER 2019:2460–71

FIGURE 1 **The STARD Diagram**

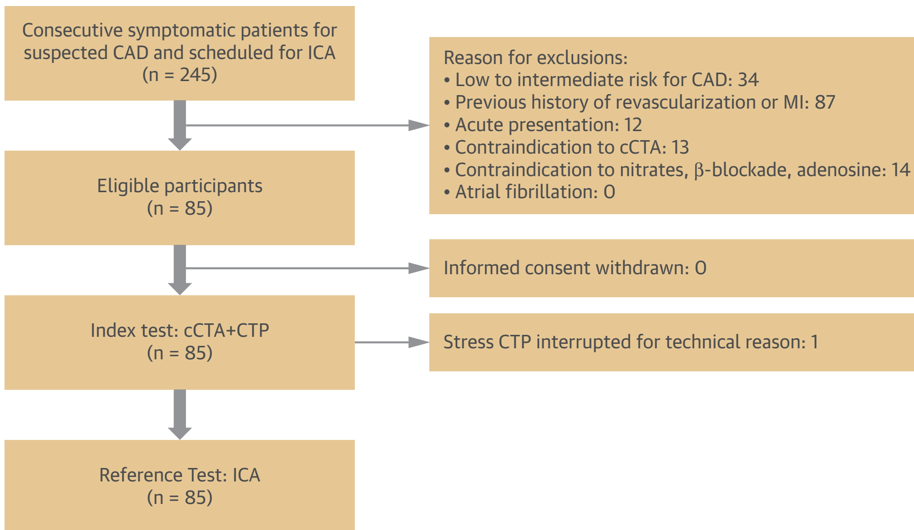

Diagram reporting the flow of participants through the study. CAD = coronary artery disease; cCTA = coronary computed tomography angiography; CTP = computed tomography perfusion; ICA = invasive coronary angiography.

was induced with an intravenous adenosine injection (0.14 mg/kg/min over 4 min). At the end of the third minute of the adenosine infusion, 0.7 ml/kg of iodixanol 320 (Visipaque 320 mg/ml, GE Healthcare, Oslo, Norway) at an infusion rate of 5 ml/s followed by 0.5 ml/kg of saline solution at an infusion rate of 5 ml/s was injected and at the same time the stress CTP acquisition was performed in free breathing. Three consecutive series of datasets were acquired covering the base of heart to the apex as shown in Figure 2.

Multiple short-axis views of the left ventricle from the base to the apex corrected for breathing-related displacement were generated and endocardial and epicardial borders were selected. Accordingly, the change of attenuation in the myocardium over time was computed. For quantification of myocardial blood

FIGURE 2 **Dynamic Stress CTP Acquisition Protocol**

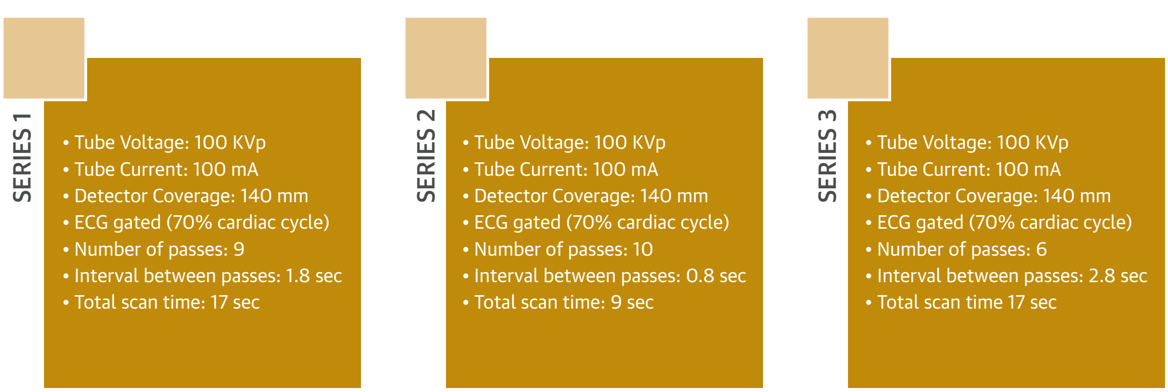

Abbreviation as in Figure 1.

flow (MBF), the arterial input function (AIF) was sampled in the ascending aorta and the myocardial time/attenuation curves were coupled with the AIF using a hybrid deconvolution model (Supplemental Appendix). Finally, MBF was computed by dividing the convoluted maximal slope of the myocardial time-attenuation curve by the maximum AIF as previously described (24). MBF maps were reconstructed as a stack of color-coded images with a slice thickness of 3.0 mm. Measurements of MBF were obtained from regions of interest of at least 1,000 pixels (i.e., at least 0.5 cm^2) positioned in a representative area of each myocardial segment according to a standard 16-segment model. Blinded adjudication was performed to verify co-registration of CTP-defined perfusion defects with culprit vessels as defined using cCTA by 2 cardiac radiologists (A.B. and G.P.) who had more than 5 years of experience, as previously described (21).

FFR_{CT} PERFORMANCE AND INTERPRETATION. All cCTA datasets were sent to HeartFlow (Redwood City, California) for FFR_{CT} analysis. An FFR_{CT} <0.80 was considered significant.

EVALUATION OF cCTA COMBINED WITH FFR_{CT} OR DYNAMIC STRESS CTP. All coronary artery imaging datasets were combined with stress CTP according to the following interpretation: 1) non-obstructive CAD was considered negative regardless of functional test findings; 2) obstructive CAD with negative functional test findings was considered negative; and 3) obstructive CAD with positive matched functional test findings was deemed positive.

EVALUATION OF cCTA COMBINED WITH FFR_{CT} AND DYNAMIC STRESS CTP. A stepwise diagnostic workup based on the sequential strategy of cCTA+FFR_{CT}+CTP was developed as follows: 1) non-obstructive CAD was considered negative regardless of functional test findings; 2) obstructive CAD with FFR_{CT} >0.8 was considered negative regardless of CTP findings; 3) obstructive CAD with FFR_{CT} <0.7 was considered positive regardless of CTP findings; and 4) obstructive CAD with FFR_{CT} between 0.7 and 0.8 was considered positive only in case of pathological CTP.

ICA AND INVASIVE FFR PERFORMANCE AND INTERPRETATION. In all patients, certified interventional cardiologists performed ICA within 60 days after the cCTA examination (25). Coronary angiograms were analyzed at the clinical site by an interventional cardiologist who was blinded to cCTA and stress CTP findings.

The severity of coronary stenosis was quantified in two orthogonal planes by identifying the minimum diameter and reference diameter for all stenosis, and the percentage of stenosis was derived. The functionally significant CAD was considered as reference according to the following definition: presence of coronary artery stenoses ≥80% or totally occluded vessels or intermediate stenoses with invasive FFR ≤0.8 (26,27).

RADIATION EXPOSURE. The effective radiation dose (ED) was calculated as the product between dose-length product and a conversion coefficient for the chest (K = 0.014 mSv/mGy × cm). For ICA, ED was calculated by multiplying the dose area product by a conversion factor (K = 0.21 mSv/mGy × cm^2) for lateral and posterior-anterior radiation exposure in the chest.

STATISTICAL ANALYSIS. Statistical analysis was performed with dedicated software SPSS version 22.0 (IBM SPSS Statistics, IBM Corporation, Armonk, New York) and R version 2.15.2. Continuous variables are expressed as mean ± SD, and discrete variables are expressed as absolute numbers and percentages. The diagnostic performance of rest cCTA alone and the combination of rest cCTA plus functional tests were measured. Regarding stress CTP, the best cut-off of MBF was identified by using maximum Youden test. The overall evaluability, sensitivity, specificity, negative predictive value, and positive predictive value were calculated versus ICA and invasive FFR. To account for repeated and potentially correlated measurements in multiple perfusion territories in a patient, generalized estimating equations were used with an exchangeable working correlation matrix for comparisons of positive and negative outcomes. The area under the curve (AUC) was measured for each strategy and compared by using DeLong test. A p value <0.05 was considered significant.

RESULTS

The study population consisted of 85 patients and the patient clinical characteristics are summarized in Table 1. The prevalence of obstructive CAD at ICA was 77% (65 of 85 patients) and the prevalence of functionally significant CAD was 57% (48 of 85 patients).

Rest cCTA was successfully performed in all patients. Fifty (59%) patients received metoprolol before the scan, with an average dose of 5.8 ± 6.5 mg, and reached a HR during the scan of 60.2 ± 8.1 beats/min (Table 1). The mean Likert score was 3.9 ± 0.5 corresponding to an overall evaluability of native coronary arteries of 98% (1,241 of 1,264 coronary artery

TABLE 1 Characteristics of the Study Population

Baseline characteristics	
N	85
Age, yrs	64.6 ± 8.2
Male	67 (79)
BMI, kg/m^2	26.7 ± 4.8
Risk factors	
Hypertension	65 (77)
Smoker	39 (46)
Hyperlipidemia	59 (69)
Diabetes	16 (19)
Family history of coronary artery disease	51 (60)
Reasons for invasive coronary angiography	
Symptoms and/or equivocal stress test	51 (60)
Positive exercise-ECG stress test	19 (22)
Positive stress echocardiography	2 (2)
Positive single-photon emission tomography	10 (12)
Positive stress cardiac magnetic resonance	3 (4)
MDCT scan protocol, rest	
HR before scanning (beats/min)	67.6 ± 10.8
β-blocker	50 (59)
β-blocker dosage (mg)	5.82 ± 6.5
HR during scanning (beats/min)	60.2 ± 8.1
Dose length product (mGy-cm)	202.1 ± 88.6
Effective dose (mSv)	2.8 ± 1.2
MDCT scan protocol, stress	
HR during scanning (beats/min)	86.5 ± 13.1
Dose length product (mGy/cm)	384.3 ± 53.1
Effective dose (mSv)	5.3 ± 0.7
Prevalence of obstructive CAD (≥50%) at ICA	
No disease	20 (23)
1-vessel disease	35 (41)
2-vessel disease	16 (19)
3-vessel disease	14 (17)
Patients	63 (74)
Prevalence of functionally significant CAD*	
No disease	37 (43)
1-vessel disease	24 (28)
2-vessel disease	14 (16)
3-vessel disease	10 (12)
Patients	48 (56)

Values are mean ± SD or n (%). *Stenosis >80% or FFR <0.8 in intermediate stenosis 30% to 80%.

BMI = body mass index; CAD = coronary artery disease; ECG = electrocardiogram; HR = heart rate; ICA = invasive coronary angiography; MDCT = multidetector computed tomography.

segments). Seventy-one of 85 patients (83%) showed obstructive CAD at cCTA. The diagnostic performance of rest cCTA is presented in Table 2. cCTA alone demonstrated a per-vessel sensitivity, specificity, negative predictive value, positive predictive value, and accuracy of 83%, 66%, 89%, 54%, and 71%, respectively.

The FFR_{CT} was successfully performed in 95% of patients (81 of 85 patients). The diagnostic performance of rest cCTA+FFR_{CT} is presented in Table 2, showing a per-vessel sensitivity, specificity, negative predictive value, positive predictive value, and accuracy of 86%, 75%, 93%, 60%, and 78%, respectively. Among patients with obstructive CAD at cCTA, the FFR_{CT} fell in the gray zone ranging between 0.7 to 0.8 in 25 left anterior descending coronary arteries, in 8 left circumflex coronary arteries, and in 8 right coronary arteries.

Stress CTP was successfully performed in all patients with a mean HR during the stress scan of 86.5 ± 13.1 beats/min (Table 1). One stress CTP was not included in our quantitative analysis of MBF due to a post-processing software error in the co-registration of the dataset. Among the remaining 84 patients, the mean absolute MBF values for ischemic territories was significantly lower as compared with normal territories (96 ± 32 ml/100 g/min vs. 130 ± 46 ml/100 g/min; $p = 0.0001$). The optimal threshold for absolute MBF to identify functionally significant CAD using the maximum Youden test was 101 ml/100 g/min. Using this threshold of MBF and based on the pre-specified diagnostic algorithm, the addition of dynamic stress CTP on top of rest cCTA demonstrated a per-vessel sensitivity, specificity, negative predictive value, positive predictive value, and accuracy of 73%, 86%, 87%, 72%, and 82%, respectively (Table 3).

Finally, the integrated model of cCTA+FFR_{CT}+stress CTP according to the pre-defined model showed a per-vessel sensitivity, specificity, negative predictive value, positive predictive value, and accuracy of 79%, 90%, 91%, 78%, and 87%, respectively.

Both the addition of FFR_{CT} and CTP improves the AUC (0.876 and 0.878, respectively) as compared with cCTA alone (0.826; $p < 0.05$). The sequential strategy of cCTA+FFR_{CT}+CTP showed the highest AUC (0.919; $p < 0.05$) as compared with all other strategies (Figure 3). The mean ED for cCTA and stress CTP was 2.8 ± 1.2 and 5.3 ± 0.7, respectively (Table 1). Representative case examples are illustrated in Figures 4 to 6.

DISCUSSION

The main finding of our study is that the addition of quantitative stress dynamic CTP significantly improves diagnostic performance of cCTA to detect functionally significant CAD and it is comparable to the addition of FFR_{CT}. Moreover, a sequential strategy based on cCTA followed by FFR_{CT} and stress dynamic CTP is associated with the highest performance with the aim to provide both anatomic and functional information (Central Illustration) (28). Of note, the ED for

TABLE 2 Comparison of Diagnostic Accuracy of cCTA, cCTA+FFR_{CT}, and cCTA+CTP in Detecting Functionally Significant CAD

Vessel-Based Analysis	cCTA	cCTA+FFR_{CT}	cCTA+CTP	cCTA+FFR_{CT}+CTP
True-positive	68	62	59	56
True-negative	114	126	142	145
False-positive	59	42	23	16
False-negative	14	10	22	15
Sensitivity	83 (75-91)	86 (78-94)	73 (63-83)	79 (69-88)
Specificity	66 (59-73)	75 (68-82)	86 (81-91)	90 (85-95)
Negative predictive value	89 (84-94)	93 (88-97)	87 (81-92)	91 (86-95)
Positive predictive value	54 (45-62)	60 (50-69)	72 (62-82)	78 (68-87)
Accuracy	71 (66-77)	78 (68-82)	82 (77-87)	87 (82-91)

Values are n or % (95% confidence interval).

CAD = coronary artery disease; cCTA = coronary computed tomography angiography; CI = confidence interval; CTP = computed tomography perfusion; FFR_{CT} = fractional flow reserve computed tomography derived.

dynamic stress CTP was 5.3 mSv, which is approximately 50% less than the ED reported in the literature.

Despite several traditional stress imaging test showed an excellent diagnostic accuracy (29), in the Dan-NICAD (Diagnosing coronary artery disease after a positive coronary computed tomography angiography study) study, 392 patients with obstructive CAD on cCTA were randomized to cardiac magnetic resonance or a nuclear stress test and further evaluated with ICA and invasive FFR when clinically indicated showing a very low sensitivity of 41% and 36%, respectively (5). One of the potential explanations is that, once a patient is identified with obstructive CAD using cCTA, we select a population having less diffuse disease, which may cause smaller areas of ischemia and increase the risk of underdiagnosis.

A recent meta-analysis on hybrid cardiac imaging combining cCTA and myocardial perfusion (30) showed improved discrimination for hybrid imaging beyond cCTA alone, on a per-vessel basis (AUC: 0.97 vs. 0.93; p = 0.047).

On the contrary, the PACIFIC trial (31) showed that positron emission tomography (PET) perfusion imaging had the best agreement with FFR-defined stenosis (sensitivity 87% and specificity 84%) and the hybrid diagnostic approach did not add incremental diagnostic value beyond stand-alone imaging. This discrepancy could be explained by the varying diagnostic performance to detect ischemia, which is higher for PET and lower for single-photon emission computed tomography (SPECT) imaging (32). However, PET is expensive and less available than CT.

Some single-center studies have tested the diagnostic performance of dynamic CTP alone or on top of cCTA.

FIGURE 3 Receiver-Operating Characteristic Curve

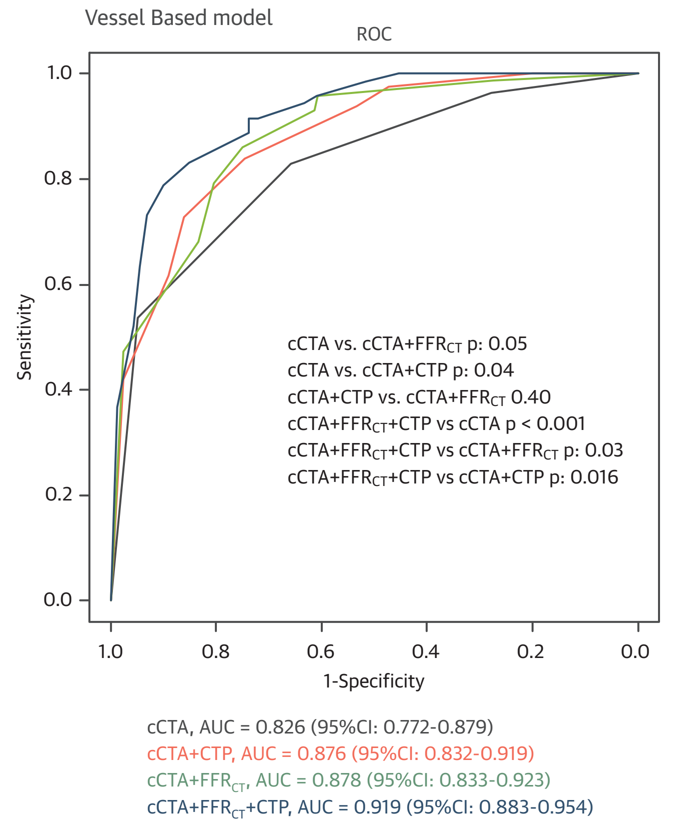

Analysis of diagnostic accuracy per vessel of cCTA alone or integrated evaluation of cCTA+FFR_{CT}, cCTA+CTP, or cCTA+FFR_{CT}+CTP to detect functionally significant CAD vs. invasive evaluation as reference standard. AUC = area under the curve; CI = confidence interval; FFR_{CT} = fractional flow reserve CT derived; ROC = receiver operating characteristics; other abbreviations as in Figure 1.

FIGURE 4 Clinical Case #1

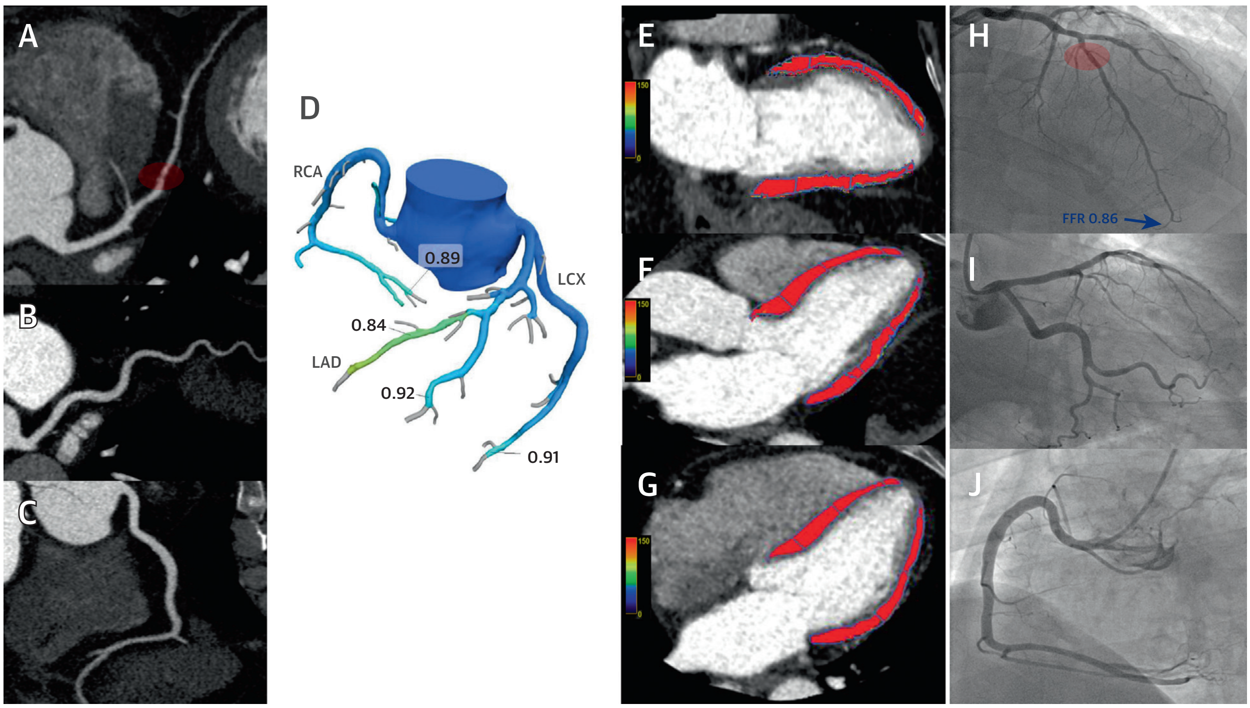

A 63-year-old man with family history of CAD, hypertension, dyslipidemia, former smoker, symptomatic for atypical angina. **(A to C)** Rest cCTA showing moderate stenosis of mid LAD **(A)**, and absence of relevant stenoses in LCx **(B)** and RCA **(C)**. **(D)** FFR_{CT} showed normal values. **(E to G)** Dynamic Stress CTP long axes view, showing absence of inducible ischemia. **(H to J)** ICA showing moderate mid-LAD stenosis with negative invasive FFR and normal LCx and RCA. LAD = left anterior descending artery; LCx = left circumflex artery; RCA = right coronary artery; FFR = fractional flow reserve; other abbreviations as in Figures 1 and 3.

Ho et al. (6) demonstrated that stress and rest dynamic perfusion imaging can detect myocardial perfusion defects with good diagnostic accuracy when compared with SPECT (per segment sensitivity, specificity, positive predictive value, and negative predictive value of 83%, 78%, 79%, and 82%, respectively) and with ICA (per-segment sensitivity, specificity, positive predictive value, and negative predictive value of 95%, 65%, 78%, and 79%, respectively). However, it should be noted that the radiation dose for this protocol was about 20 mSv.

Bastarrika et al. (7) compared dynamic CT perfusion with cardiac magnetic resonance imaging in 10 patients. Sensitivity, specificity, positive predictive value, and negative predictive value for detection of perfusion defects at CT were 86%, 98%, 94%, and 96%, respectively.

Rossi et al. (13) performed CT coronary angiography and dynamic CT perfusion imaging in 80 patients who had stable chest pain and they found that the optimal cutoff value for detection of hemodynamically significant coronary stenosis was 78 mL/100 mL/min. In addition, the authors demonstrated that, in the group of patients with intermediate coronary stenosis (30% to 70% lumen narrowing as defined at CT coronary angiography), the subsequent use of dynamic CT perfusion imaging significantly improved the specificity of visual and quantitative CT coronary angiography compared with FFR.

Bamberg et al. (33) showed good diagnostic performance using a MBF threshold of 88 ml/100 g/min on dynamic CTP for the detection of any perfusion defect), reporting a sensitivity of 77.8% and a negative predictive value of 91.3% with moderate positive predictive value and specificity of 51% and 75%, respectively.

Using a mean MBF of 79 ml/100 ml/min, Coenen et al. (18) demonstrated a diagnostic accuracy and

FIGURE 5 Clinical Case #2

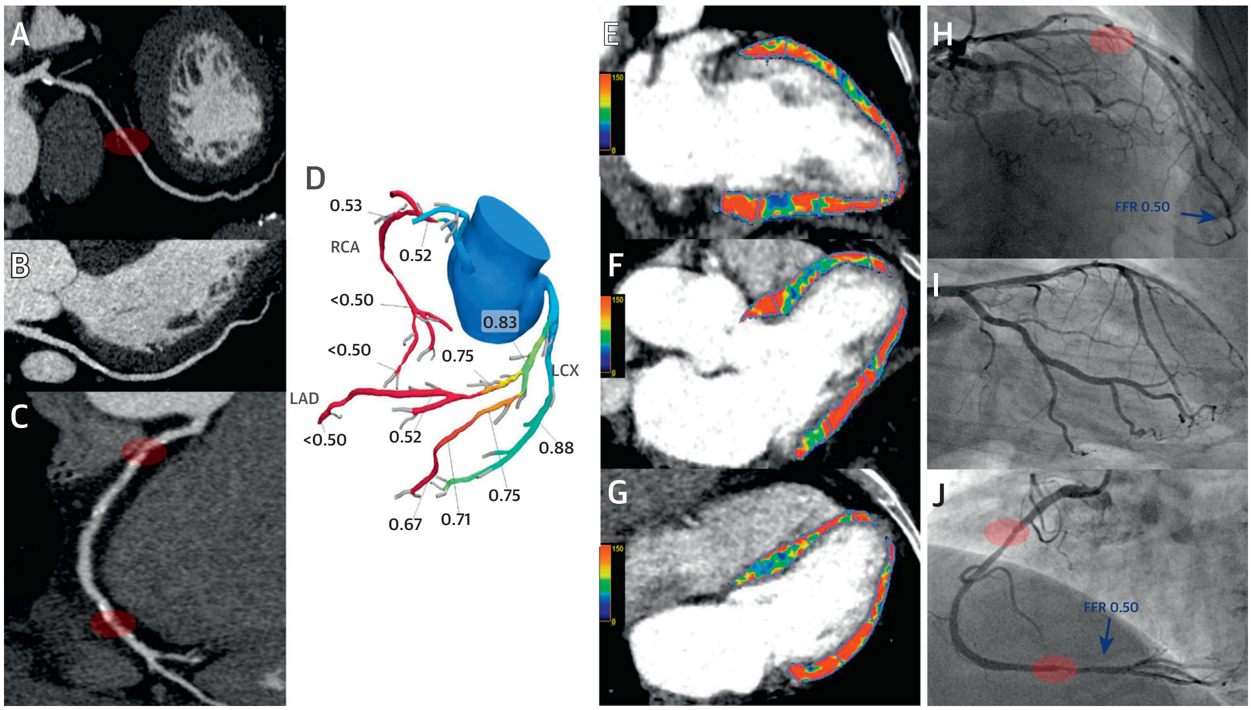

A 63-year-old man with family history of CAD, hypertension, diabetes, former smoker, atypical angina, and recent exercise electrocardiogram and SPECT both inconclusive for inducible ischemia. **(A to C)** Rest cCTA showing severe stenosis of mid-LAD **(A)**, absence of relevant stenoses of LCx **(B)**, and severe stenoses of proximal and distal RCA **(C)**. **(D)** FFR_{CT} showed positive values for LAD and RCA. **(E to G)** Dynamic Stress CTP long-axes views showing diffuse ischemia. **(H to J)** ICA showing severe stenosis of mid-LAD with positive FFR, normal LCX, and severe stenoses of proximal and distal RCA with positive FFR value. Abbreviations as in Figures 1, 3, and 4.

AUC for stress dynamic CTP of 68% and 0.75, respectively. When MBF was integrated to cCTA, the diagnostic accuracy significantly improved to 77%. Of note, the mean radiation dose was 9.3 ± 1.8 mSv.

More recently, Lu et al. (34) published a meta-analysis on dynamic CTP showing pooled sensitivity and specificity of 85% and 81% at the vessel level, respectively, and 93% and 82% at the patient level, respectively.

Some preliminary studies testing the accuracy of dynamic CTP with whole-heart CT coverage scanner were also performed versus PET (15). Kikuchi et al. (15) showed a strong correlation between MBF as detected using cCTA and PET ($r = 0.67$; $p = 0.0126$) in healthy volunteers.

STUDY STRENGTHS AND LIMITATIONS. Our study shows some strengths. It was prospective in nature where the stress dynamic CTP was performed per protocol and all patients underwent invasive evaluation avoiding any referral bias. The combination of ICA plus invasive FFR when appropriate was used, overcoming the limitation of the majority of previous studies where mainly ICA alone was used. Importantly, compared with previous studies, we found a higher diagnostic accuracy with an approximate 50% reduction of ED. To this regard, Enjilela et al. (35) reported a compressed sensing technique to reduce the overall effective dose in dynamic CTP in a pig model reaching an effective dose around 2.7 mSv but the main limitation of this technique is the computationally intensive image reconstruction compared with the standard dynamic CTP approach.

Of note, according to the previous experiences with dynamic CTP, the MBF value measured in our study is different as compared with the values measured using PET that are 3 to 4 times higher (36). The potential explanation is that the myocardial extraction of iodine contrast agent is partial and influenced by flow rate (36). Indeed, MBF measured with dynamic CTP reflects the transfer constant from the blood compartment to the tissue

JACC: CARDIOVASCULAR IMAGING, VOL. 12, NO. 12, 2019
DECEMBER 2019:2460–71

FIGURE 6 Clinical Case #3

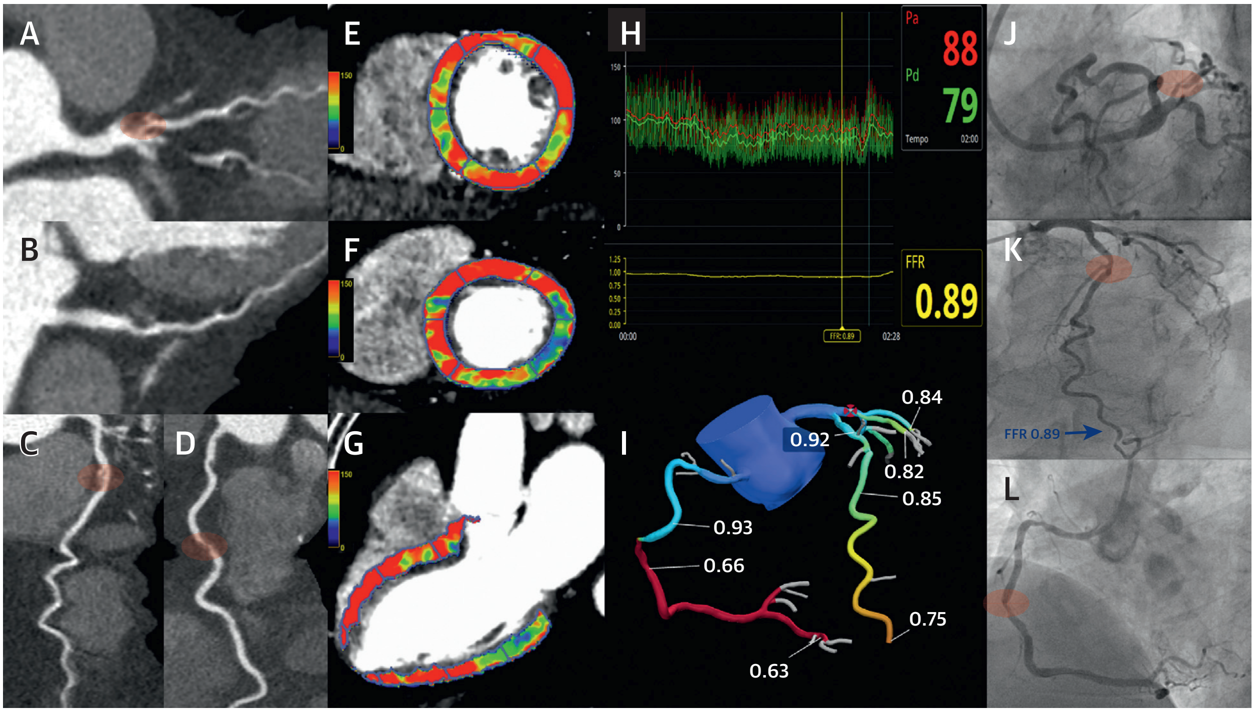

A 56-year-old man with family history positive for CAD, hypertension, smoking, ex-electrocardiogram positive for inducible ischemia. **(A to D)** Rest cCTA showing subocclusive stenosis of RI **(A and B)**, moderate stenosis of proximal LAD **(C)**, and severe stenoses of proximal and mid-RCA **(D)**. **(E and F)** Dynamic Stress CTP short axis, showing inducible ischemia of basal to mid-inferolateral wall, basal inferior wall, mid to apical inferoseptal wall, mid to apical anterolateral wall. **(G)** Dynamic Stress CTP long axis showed ischemia of basal inferior wall. **(H)** FFR plot of mid-LAD with negative value. **(I)** FFRCT positive value of RCA and distal LAD. **(J to L)** ICA showing subocclusion of RI **(J)**, moderate stenosis of mid-LAD with negative FFR **(K)**, severe stenoses of proximal and mid-RCA with positive FFR value **(L)**. Abbreviations as in Figures 1, 3, and 4.

compartment rather than the absolute value of myocardial flow. As a result, the relationship between myocardial perfusion and iodine contrast extraction is not linear, resulting in underestimation of MBF (36). Therefore, the cut-off value of stress MBF for detection of significant CAD determined using PET is not applicable to MBF calculated with dynamic CTP.

Moreover, when we tested the performance of an integrated model of cCTA plus FFR_{CT} plus stress dynamic CTP, we have considered functionally significant CAD with FFR_{CT} between 0.7 and 0.8 only in case of matched perfusion defect as detected by CTP. Indeed, despite a good correlation between FFR_{CT} with invasive FFR, slight underestimations were reported. This means that in the intermediate range, however, a substantially lower diagnostic accuracy of 46% has been shown (37). Accordingly, the concept of borderline or 'gray-zone' FFRct results has been introduced, emphasizing that particularly in these cases of values further management should be performed. As shown in our model, integrating dynamic CTP in this setting, the diagnostic accuracy is significantly improved.

Despite stress dynamic CTP and FFR_{CT} showed similar diagnostic performance, their applicability could be different based on the advantages of each technique. For example, CTP is based on on-site interpretation, it is independent of coronary artery interpretability, it can be applied to patients with previous revascularization, and finally it is useful also in case of microcirculatory disease. Different from CTP, FFR_{CT} needs only single rest scan and stress agent is not required. Therefore, it is useful for patients with contraindication to stressor or

CENTRAL ILLUSTRATION Potential Diagnostic Algorithm to Select Patients With Suspected CAD Who May Derive Benefit by ICA and Consequent Revascularization

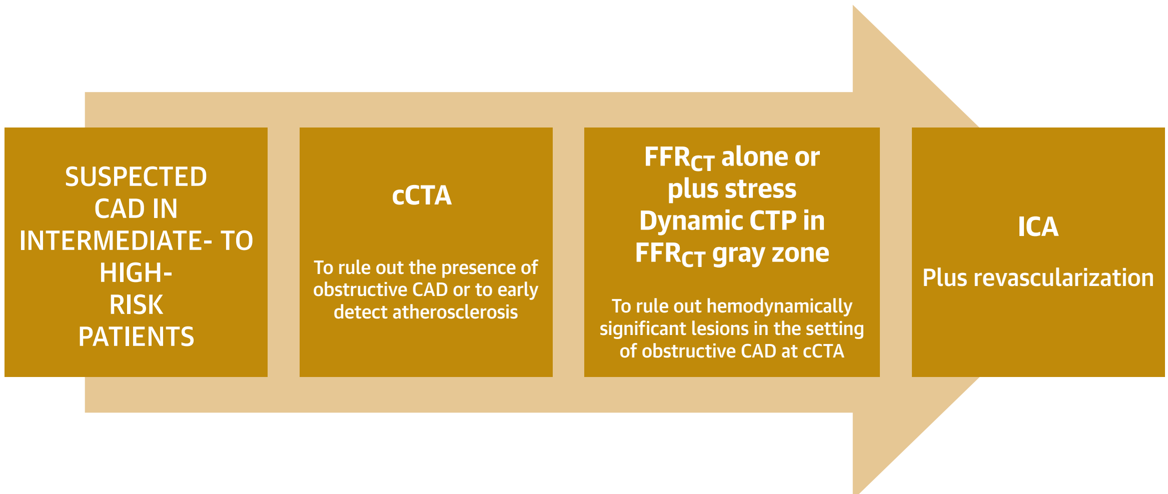

Pontone, G. et al. J Am Coll Cardiol Img. 2019;12(12):2460–71.

CAD = coronary artery disease; cCTA = coronary computed tomography angiography; FFR_{CT} = fractional flow reserve computed tomography derived; ICA = invasive coronary angiography; CTP = stress myocardial computed tomography perfusion.

young patients in whom the radiation exposure needs to be held as low as possible.

Some limitations are present in this study. First, we have included patients scheduled for ICA and this could be responsible for a potential inclusion bias and invasive FFR was not performed in all vessels but only in intermediate lesions. However, this method is in agreement with accepted clinical standards. Second, despite ED being lower as compared with previous studies, the cumulative ED for coronary artery imaging and MBF estimation is not negligible. Moreover, our study protocol for coronary artery imaging was not focused on radiation exposure reduction, and a further decrease of ED can be achieved by using a single cardiac phase acquisition rather than a multiphase acquisition during rest acquisition. Third, our results can be applied only in patients with the same prevalence of functionally significant CAD. Finally, the MBF cut-off used in our study to define the presence of functionally significant CAD was derived and it was slightly higher as compared with previous studies. However, in general, the absolute value of MBF as detected using stress dynamic CTP should be taken with caution because it could be partly related to differences in patient characteristics, technical factors related to image quality, modeling of contrast agent kinetics, temporal resolution of acquisition, and flow rate of contrast injection. Therefore, a definitive cut-off value of stress MBF for detection of significant CAD is not still determined and large databases of normal perfusion values incorporating different scan protocols are highly desirable.

CONCLUSIONS

In patients with suspected CAD at intermediate to high risk, the addition of quantitative dynamic stress CTP is associated with a high diagnostic accuracy and low radiation exposure. Further studies to test the cost-effectiveness of this strategy as compared with a pure anatomical or functional approach are warranted.

ADDRESS FOR CORRESPONDENCE: Dr. Gianluca Pontone, Centro Cardiologico Monzino, IRCCS, Via C. Parea 4, 20138 Milan, Italy. E-mail: gianluca.pontone@ccfm.it. Twitter: @gpontone1.

JACC: CARDIOVASCULAR IMAGING, VOL. 12, NO. 12, 2019
DECEMBER 2019:2460–71

PERSPECTIVES

COMPETENCY IN MEDICAL KNOWLEDGE: There is an emerging literature on the added value of FFR_{CT} and stress CTP on top of cCTA in patients with obstructive CAD. The rationale behind this approach is that both FFR_{CT} and myocardial CTP can provide functional data when the cCTA images reveal borderline lesions or when coronary segments are difficult to interpret because of dense calcium. On the other hand, cCTA images can be useful to determine false-positive FFR_{CT} value or false-positive perfusion defects. Initial single-center studies with stress dynamic CTP were performed with shuttle-mode approach. However, this approach is associated with high radiation exposure and few comparative data exist between dynamic CTP and FFR_{CT}. The aim of our study was to test the diagnostic accuracy of an integrated evaluation of cCTA plus FFR_{CT} plus dynamic CTP using a whole-heart coverage CT scanner compared with ICA plus invasive FFR to detect the functional relevance of CAD.

TRANSLATIONAL OUTLOOK: The main finding of our study is that the addition of quantitative stress dynamic CTP to integrated evaluation of cCTA+FFR_{CT} significantly improves diagnostic performance to detect functionally significant CAD as compared with cCTA alone. Of note, the ED for dynamic stress CTP requires just 5.3 mSv that is approximately 50% less than the ED reported in the literature for dynamic CTP. To the best of our knowledge, this is the first study that prospectively tested the incremental value of this dynamic CTP protocol. A sequential strategy based on cCTA followed by FFR_{CT} and myocardial perfusion imaging has the ability to provide a full overview of anatomical and functional aspects of CAD.

REFERENCES

1. Pontone G, Andreini D, Quaglia C, Ballerini G, Nobili E, Pepi M. Accuracy of multidetector spiral computed tomography in detecting significant coronary stenosis in patient populations with differing pre-test probabilities of disease. Clin Radiol 2007;62:978–85.

2. Schulman-Marcus J, Hartaigh BO, Gransar H, et al. Sex-specific associations between coronary artery plaque extent and risk of major adverse cardiovascular events: the CONFIRM long-term registry. J Am Coll Cardiol Img 2016;9:364–72.

3. Pontone G, Andreini D, Bartorelli AL, et al. A long-term prognostic value of CT angiography and exercise ECG in patients with suspected CAD. J Am Coll Cardiol Img 2013;6:641–50.

4. Pontone G, Bertella E, Mushtaq S, et al. Coronary artery disease: diagnostic accuracy of CT coronary angiography–a comparison of high and standard spatial resolution scanning. Radiology 2014;271:688–94.

5. Nissen L, Winther S, Westra J, et al. Diagnosing coronary artery disease after a positive coronary computed tomography angiography: the Dan-NICAD open label, parallel, head to head, randomized controlled diagnostic accuracy trial of cardiovascular magnetic resonance and myocardial perfusion scintigraphy. Eur Heart J Cardiovasc Img 2018;19:369–77.

6. Ho KT, Chua KC, Klotz E, Panknin C. Stress and rest dynamic myocardial perfusion imaging by evaluation of complete time-attenuation curves with dual-source CT. J Am Coll Cardio Img 2010;3: 811–20.

7. Bastarrika G, Ramos-Duran L, Rosenblum MA, Kang DK, Rowe GW, Schoepf UJ. Adenosine-stress dynamic myocardial CT perfusion imaging: initial clinical experience. Invest Radiol 2010;45:306–13.

8. Bamberg F, Becker A, Schwarz F, et al. Detection of hemodynamically significant coronary artery stenosis: incremental diagnostic value of dynamic CT-based myocardial perfusion imaging. Radiology 2011;260:689–98.

9. Wang Y, Qin L, Shi X, et al. Adenosine-stress dynamic myocardial perfusion imaging with second-generation dual-source CT: comparison with conventional catheter coronary angiography and SPECT nuclear myocardial perfusion imaging. AJR Am J Roentgenol 2012; 198:521–9.

10. Weininger M, Schoepf UJ, Ramachandra A, et al. Adenosine-stress dynamic real-time myocardial perfusion CT and adenosine-stress first-pass dual-energy myocardial perfusion CT for the assessment of acute chest pain: initial results. Eur J Radiol 2012;81:3703–10.

11. Huber AM, Leber V, Gramer BM, et al. Myocardium: dynamic versus single-shot CT perfusion imaging. Radiology 2013;269:378–86.

12. Kim SM, Choi JH, Chang SA, Choe YH. Detection of ischaemic myocardial lesions with coronary CT angiography and adenosine-stress dynamic perfusion imaging using a 128-slice dual-source CT: diagnostic performance in comparison with cardiac MRI. Br J Radiol 2013;86:20130481.

13. Rossi A, Dharampal A, Wragg A, et al. Diagnostic performance of hyperaemic myocardial blood flow index obtained by dynamic computed tomography: does it predict functionally significant coronary lesions? Eur Heart J Cardiovasc Img 2014;15:85–94.

14. Kono AK, Coenen A, Lubbers M, et al. Relative myocardial blood flow by dynamic computed tomographic perfusion imaging predicts hemodynamic significance of coronary stenosis better than absolute blood flow. Invest Radiol 2014;49:801–7.

15. Kikuchi Y, Oyama-Manabe N, Naya M, et al. Quantification of myocardial blood flow using dynamic 320-row multi-detector CT as compared with (1)(5)O-H(2)O PET. Eur Radiol 2014;24: 1547–56.

16. Ebersberger U, Marcus RP, Schoepf UJ, et al. Dynamic CT myocardial perfusion imaging: performance of 3D semi-automated evaluation software. Eur Radiol 2014;24:191–9.

17. Tanabe Y, Kido T, Uetani T, et al. Differentiation of myocardial ischemia and infarction assessed by dynamic computed tomography perfusion imaging and comparison with cardiac magnetic resonance and single-photon emission computed tomography. Eur Radiol 2016;26:3790–801.

18. Coenen A, Rossi A, Lubbers MM, et al. Integrating CT myocardial perfusion and CT-FFR in the work-up of coronary artery disease. J Am Coll Cardiol Img 2017;10:760–70.

19. Genders TS, Steyerberg EW, Alkadhi H, et al. A clinical prediction rule for the diagnosis of coronary artery disease: validation, updating, and extension. Eur Heart J 2011;32:1316–30.

20. Bossuyt PM, Reitsma JB, Bruns DE, et al. STARD 2015: an updated list of essential items for reporting diagnostic accuracy studies. Radiology 2015;277:826–32.

21. Pontone G, Andreini D, Guaricci AI, et al. Incremental diagnostic value of stress computed tomography myocardial perfusion with whole-heart coverage CT scanner in intermediate- to high-risk symptomatic patients suspected of coronary artery disease. J Am Coll Cardiol Img 2019;12:338–49.

22. Leipsic J, Abbara S, Achenbach S, et al. SCCT guidelines for the interpretation and reporting of coronary CT angiography: a report of the Society of Cardiovascular Computed Tomography Guidelines Committee. J Cardiovasc Computed Tomography 2014;8:342–58.

23. Austen WG, Edwards JE, Frye RL, et al. A reporting system on patients evaluated for coronary artery disease. Report of the Ad Hoc Committee for Grading of Coronary Artery Disease, Council on Cardiovascular Surgery, American Heart Association. Circulation 1975;51:5–40.

24. Rossi A, Merkus D, Klotz E, Mollet N, de Feyter PJ, Krestin GP. Stress myocardial perfusion: imaging with multidetector CT. Radiology 2014;270:25–46.

25. Levine GN, Bates ER, Blankenship JC, et al. 2011 ACCF/AHA/SCAI Guideline for Percutaneous Coronary Intervention. A report of the American College of Cardiology Foundation/American Heart Association Task Force on Practice Guidelines and the Society for Cardiovascular Angiography and Interventions. J Am Coll Cardiol 2011;58:e44–122.

26. Tonino PA, De Bruyne B, Pijls NH, et al. Fractional flow reserve versus angiography for guiding percutaneous coronary intervention. N Engl J Med 2009;360:213–24.

27. De Bruyne B, Pijls NH, Kalesan B, et al. Fractional flow reserve-guided PCI versus medical therapy in stable coronary disease. N Engl J Med 2012;367:991–1001.

28. Pontone G. Anatomy and physiology in ischaemic heart disease: a second honeymoon? Eur Heart J 2016;37:1228–31.

29. Greenwood JP, Maredia N, Younger JF, et al. Cardiovascular magnetic resonance and single-photon emission computed tomography for diagnosis of coronary heart disease (CE-MARC): a prospective trial. Lancet 2012;379:453–60.

30. Rizvi A, Han D, Danad I, et al. Diagnostic performance of hybrid cardiac imaging methods for assessment of obstructive coronary artery disease compared with stand-alone coronary computed tomography angiography: a meta-analysis. J Am Coll Cardiol Img 2018;11:589–99.

31. Danad I, Raijmakers PG, Driessen RS, et al. Comparison of coronary CT angiography, SPECT, PET, and hybrid imaging for diagnosis of ischemic heart disease determined by fractional flow reserve. JAMA Cardiol 2017;2:1100–7.

32. Danad I, Szymonifka J, Twisk JWR, et al. Diagnostic performance of cardiac imaging methods to diagnose ischaemia-causing coronary artery disease when directly compared with fractional flow reserve as a reference standard: a meta-analysis. Eur Heart J 2017;38:991–8.

33. Bamberg F, Marcus RP, Becker A, et al. Dynamic myocardial CT perfusion imaging for evaluation of myocardial ischemia as determined by MR imaging. J Am Coll Cardiol Img 2014;7:267–77.

34. Lu M, Wang S, Sirajuddin A, Arai AE, Zhao S. Dynamic stress computed tomography myocardial perfusion for detecting myocardial ischemia: a systematic review and meta-analysis. Int J Cardiol 2018;258:325–31.

35. Enjilela E, Lee TY, Hsieh J, et al. Ultra-low dose quantitative CT myocardial perfusion imaging with sparse-view dynamic acquisition and image reconstruction: a feasibility study. Int J Cardiol 2018;254:272–81.

36. Ishida M, Kitagawa K, Ichihara T, et al. Underestimation of myocardial blood flow by dynamic perfusion CT: explanations by two-compartment model analysis and limited temporal sampling of dynamic CT. J Cardiovasc Computed Tomography 2016;10:207–14.

37. Cook CM, Petraco R, Shun-Shin MJ, et al. Diagnostic accuracy of computed tomography-derived fractional flow reserve: a systematic review. JAMA Cardiol 2017;2:803–10.

KEY WORDS accuracy, computed tomography, coronary artery disease, dynamic stress computed tomography

APPENDIX For supplemental information, please see the online version of this paper.